applied sciences

MDPI

Article

Fall Risk Assessment in Active Elderly Through the Use of Inertial Measurement Units: Determining the Right Postural Balance Variables and Sensor Locations

Youssef Nkizi and Ornwipa Thamsuwan *

Department of Mechanical Engineering, École de Technologie Supérieure, Montreal, QC H3C 1K3, Canada
* Correspondence: ornwipa.thamsuwan@etsmtl.ca

Abstract: Falls among the elderly have been a significant public health challenge, with severe consequences for individuals and healthcare systems. Traditional balance assessment methods often lack ecological validity, necessitating more comprehensive and adaptable evaluation techniques. This research explores the use of inertial measurement units to assess postural balance in relation to the Berg Balance Scale outcomes. We recruited 14 participants from diverse age groups and health backgrounds, who performed 14 simulated tasks while wearing inertial measurement units on the head, torso, and lower back. Our study introduced a novel metric, i.e., the volume that envelops the 3-dimensional accelerations, calculated as the convex hull space, and used this metric along with others defined in previous studies. Through logistic regression, we demonstrated significant associations between various movement characteristics and the instances of balance loss. In particular, greater movement volume at the lower back (p = 0.021) was associated with better balance, while root-mean-square lower back angular velocity (p = 0.004) correlated with poorer balance. This study revealed that sensor location and task type (static vs. dynamic) significantly influenced the coefficients of the logistic regression model, highlighting the complex nature of balance assessment. These findings underscore the potential of IMUs in providing detailed objective balance assessments in the elderly by identifying specific movement patterns associated with balance impairment across various contexts. This knowledge can guide the development of targeted interventions and strategies for fall prevention, potentially improving the quality of life for older adults.

Keywords: balance assessment; Berg Balance Scale; elderly; fall prevention; inertial measurement units; kinematics

Citation: Nkizi, Y.; Thamsuwan, O. Fall Risk Assessment in Active Elderly Through the Use of Inertial Measurement Units: Determining the Right Postural Balance Variables and Sensor Locations. *Appl. Sci.* **2024**, *14*, 11312. https://doi.org/10.3390/app142311312

Academic Editor: Lingfeng Shi

Received: 8 October 2024
Revised: 25 November 2024
Accepted: 26 November 2024
Published: 4 December 2024

1. Introduction

Falls among the elderly represent a significant public health concern with substantial consequences. Falls can have a devastating impact on the lives of older adults, leading to injuries, immobility, activity limitations, placement in nursing homes, health deterioration, and increased risk of mortality [1]. Research indicated that nearly all hip fractures in older adults result from falls [2], with a significant percentage leading to serious outcomes such as long-term institutionalization or death. In addition, there can also be psychosocial consequences such as the fear of falling again, increased healthcare costs, strain on family relationships, and limited social participation [3]. The costs associated with fall-related injuries are substantial. In the United States, healthcare expenses for fall-related injuries among older adults were approximately 50 billion dollars annually [4]. Additionally, as the elderly population grows, the incidence of non-fatal falls has risen significantly, increasing demand for emergency and healthcare services [4]. In 2018 alone, an estimated 3 million emergency department visits, over 950,000 hospital admissions or transfers to other facilities (e.g., trauma centers), and around 32,000 deaths were attributed to fall-related injuries among older adults [4].

Maintaining postural balance is essential for mobility, independence, and quality of life in older adults. Continuous monitoring of balance is, therefore, crucial to identify situations that may lead to increased fall risk, such that we can put preventive interventions in place before it happens. Balance assessment methods have evolved significantly over time, ranging from simple clinical observations to more advanced technological approaches. Traditional methods for evaluating balance include clinical assessments performed by physiotherapists, which involve observation of gait, posture, behavior, facial expressions, and emotional responses [5]. Traditional methods may also include functional tests such as the six-minute walk test [6], the Timed Up and Go (TUG) test [7], the Berg Balance Scale (BBS) test [8], and the Star Excursion Balance Test (SEBT) [9]. Each one was designed to evaluate different aspects of balance and mobility. However, clinical observation faces inherent limitations due to its subjective nature. Inter-observer variability is a major challenge, potentially impacting the reliability of assessments [10]. As demonstrated in a previous study using SEBT [9], there were disagreements among clinicians in identifying movement abnormalities. Despite their practicality and simplicity, these functional tests still lacked the precision and objectivity offered by more advanced techniques involving direct measurements.

The more advanced quantitative techniques that were developed and validated are force platforms [11] and motion capture systems [12] for estimating the center of pressure or mass. Force platforms have been used to measure postural sway and center of pressure movements during quiet standing and various balance tasks [11]. Motion capture systems include marker-based optical systems and markerless video-based systems, which allow for detailed analysis of body movements. Nevertheless, both clinical observations and advanced technologies primarily operate within controlled clinical environments. These methods are constrained in their ability to capture the dynamic nature of balance in real-world scenarios. Specifically, previous research highlighted a critical issue that force plate measures often exhibit a limited correlation with actual balance performance outside the laboratory [11]. Recognizing this limitation underscores the need for assessment tools that offer greater ecological validity, capable of providing metrics for postural balance assessment in everyday life situations. Considering this limitation, wearable devices that can capture similar measures may be more appropriate.

Inertial Measurement Units (IMUs), consisting of miniaturized accelerometers, gyroscopes, and magnetometers, have emerged as a promising solution. Their portability enables balance assessment in more natural settings, capturing movement data during a wider range of activities in both laboratory and real-world settings, such as residential homes, workplaces, and public spaces [13–15]. IMUs offer continuous monitoring capabilities, allowing for the detection of subtle balance fluctuations that might be missed during brief, clinically-based assessments. Previous research has demonstrated the feasibility of using IMUs to assess various aspects of balance. De Groote (2020) showed that a smartphone-embedded IMU could effectively measure postural stability, with results moderately correlating with gold-standard force platform assessments [13]. In addition, Nouredanesh and Tung (2015) explored the use of IMUs combined with machine learning to automatically detect compensatory balance responses during lateral perturbations, achieving high classification accuracy [16]. Moreover, Pickle et al. (2018) demonstrated the potential of these devices for estimating segmental contributions to total body angular momentum in individuals with Parkinson's disease, using a limited set of sensors [17]. With a large dataset and machine learning models, postural balance characteristics derived from IMU data were found to be useful. For instance, Liuzzi et al. (2023) [18] were able to evaluate the balance of stroke and Parkinson's patients from placing the IMUs on them while they performed the 6-minute walk test. Also, IMUs may be used complementarily with other sources. A study by Silva (2020) [19] combined IMU and force plate data from 403 elderly participants performing the TUG test and employed machine learning and deep learning models to predict and detect falls among older adults.

The research presented in this paper was built upon these promising findings, with the first objective to further explore the potential of IMUs for evaluating postural balance in the elderly during their daily living. Particularly, we developed a straightforward and practical protocol for using IMU sensors, including the steps of calibration, body placement, data recording, and calculation of kinematic features; then, we identified IMU-derived features that are sensitive to variations in postural balance. Our hypothesis was that the features derived from an IMU placed on the lower back will be predictive of fall risk due to its proximity to the body's center of mass and its capacity to capture overall postural oscillations.

The placement of IMUs on the body is a critical consideration in balance assessment. Previous studies have explored various sensor locations. Since securing an IMU on the lower back can be challenging in real-world settings as the person may sit or lean on it, it would be interesting to see if we can change the location of a single IMU to another body part. A systematic review by Ghislieri et al. (2019) found that the majority of studies (80.9%) place sensors in the lower back region, particularly at the L5/S1 level, which is close to the body's center of mass [20]. The use of IMUs in this location was also validated in the real-world setting; for example, among Parkinson's patients living at home [21]. Besides the L5/S1, Shin and Yoo (2019) demonstrated the importance of sacrum-placed sensors in evaluating standing posture and balance [22]. Their study revealed a strong correlation between the sacrum angle and overall lumbar lordosis, which is important in maintaining postural alignment and stability. As for other locations, Scheltinga et al. (2022) highlighted the relevance of sternum-placed sensors for estimating vertical ground reaction forces during running [23]. Last but not least, using the head as a reference was proven effective for assessing vestibular disorders [24] and vision troubles [25]. Janc et al. (2021) showed the utility of head-mounted accelerometers together with a force plate in assessing the balance of patients with vestibular disorders [24]. Depra et al. (2019) established a relationship between postural balance measured at the head and visual tracking accuracy, observing that postural stability decreased in challenging visual conditions while standing on one leg [25].

Building on this foundation, the second aim of our study was to investigate the impact of sensor placement, especially the torso and the head, on the interpretation of balance assessment results. Recognizing the complex, multi-segmental nature of balance control, our research aimed to find which sensor locations could provide the most informative data about balance performance. We compared balance parameters derived from data collected from IMUs positioned on the head, torso, and lower back.

2. Materials and Methods

2.1. Participants

Fourteen persons (6 women, 8 men) with an average age of 59 (SD 10.2) years participated in this study. The participants were recruited through a convenient sampling in an urban neighborhood, and were meant to represent the middle age (40–65 years old) as well as elderly population (65 years and above). The participants represented a diverse age range; that is, two individuals were in the 40–49 age range, seven were in the 50–59 range, four were in the 60–69 range, one was in the 70–79 range, and one was in the 80–89 range. Participants' weight ranged from 52 kg to 98 kg (average 75.13 kg, SD 15.04 kg), and height from 157 cm to 183 cm (average 170.87 cm, SD 9.20 cm).

The participants' medical history revealed a range of conditions potentially influencing balance performance. Eight participants reported vision disorders, seven had cardiovascular issues (three cardiopathy and four hypertension), and six had endocrine disorders (three diabetes and three thyroid problems). Ten participants reported respiratory conditions (seven had allergies and three had asthma). Five participants had a history of prior surgery. There were no reported cases of Parkinson's disease, hypotension or stroke.

2.2. Instruments for Data Collection

We used three IMUs (SXT, NexGen Ergonomic, Montreal, QC, Canada). Each IMU integrated tri-axial accelerometers (±16 g range), gyroscopes (±2000°/s range), and magnetometers, sampled at 128 Hz. The three IMUs were synchronized prior to the data collection.

The IMUs were positioned on the participants' head (behind the right ear), sternum, and low back at the L5/S1 level, as shown in Figure 1. The lower back placement was chosen for its proximity to the body's center of mass and reduced susceptibility to non-postural movements.

Figure 1. IMU placement locations: head (**top left**), torso (**bottom left**), and lower back (**right**).

At the beginning of the data collection, the IMU's initial state was collected when participants stood still for 10 s and was referred to as "Ipose". Median acceleration values during this pose served as reference points. The accelerations throughout the entire data collection were then subtracted from these median accelerations, as shown in Equation (1):

$$\begin{aligned} a_X &= a_{\text{raw},X} - \bar{a}_{\text{ipose},X} \\ a_Y &= a_{\text{raw},Y} - \bar{a}_{\text{ipose},Y} \\ a_Z &= a_{\text{raw},Z} - \bar{a}_{\text{ipose},Z} \end{aligned} \tag{1}$$

where a_X, a_Y, and a_Z are accelerations to be further used, $a_{\text{raw},X}$, $a_{\text{raw},Y}$, and $a_{\text{raw},Z}$ are the raw accelerations, and $\bar{a}_{\text{ipose},X}$, $\bar{a}_{\text{ipose},Y}$, and $\bar{a}_{\text{ipose},Z}$ are the median reference accelerations for each axis.

2.3. Balance Assessment Tasks

Participants performed 14 standardized tasks in the Berg Balance Scale (BBS) test [8], which is a widely used clinical tool for assessing functional balance. Through observation by two researchers, the outcome of each task was scored on an ordinal discrete scale from 0 to 4, with higher scores reflecting better balance performance. Table 1 provides a comprehensive overview of these tasks, illustrating the diverse range of balance challenges presented to the participants.

Table 1. Berg Balance Scale tasks.

Task	Description
1	Sit to stand
2	Standing unsupported
3	Sitting unsupported
4	Stand to sit
5	Transfers
6	Standing with eyes closed
7	Standing with feet together
8	Reaching forward with outstretched arm
9	Retrieving object from floor
10	Turning to look behind
11	Turning 360 degrees
12	Placing an alternate foot on stool
13	Standing with one foot in front
14	Standing on one foot

2.4. Data Processing

Data were saved and then exported from the IMU buit-in software (TK Motion Manager, NexGen Ergonomic, Montreal, QC, Canada), initially in .h5 format, then converted to .csv for analysis. A custom Python script was developed to automate data organization. This script extracted relevant data columns (time, acceleration, angular velocity), renamed files using a standardized convention (participant ID_sensor location_task_date), and organized them into a hierarchical folder structure.

To ensure data quality and reliability before calculating the parameters of interest, we implemented several pre-processing steps. First, linear interpolation was applied to replace missing values in the IMU data. Then, a 6th order Butterworth low-pass filter with a cutoff frequency of 3.667 Hz was applied to attenuate high-frequency noise while preserving significant movement components. This choice of the cutoff frequency came from its ability to remove noise in this dataset without altering the detection of movement, which was also explored through trial and error, and supported by a previous research study [26].

Additionally, BBS scores in each of the fourteen tasks, originally collected in the range from 0 to 4, were transformed. Individual task scores were dichotomized such that the scores of 0–3, indicating potential balance difficulties, were re-coded as 1 (poor balance), while the score of 4, representing good balance, was re-coded as 0 (good balance).

2.5. Postural Balance Parameters

Several characteristics from the pre-processed IMU data were calculated as follows.

2.5.1. Total Path Length

Total path length, the cumulative distance traveled by the body segment during the recording period, was calculated. First, the displacement of the body segment was obtained through double integration of the pre-processed acceleration data, as shown in Equation (2).

$$d(t) = \iint a(t)dtdt \tag{2}$$

where $a(t)$ is the acceleration and $d(t)$ is the displacement.

The total path length L is then calculated by summing the absolute displacements across the three orthogonal axes, i.e., the 3D Cartesian coordinate system (X, Y, Z), as shown in Equation (3). It is necessary to use absolute values to ensure no effect of the directions of the changes was included in the sum of the distance.

$$L = \sum |D_x| + \sum |D_y| + \sum |D_z| \tag{3}$$

where D_x, D_y, and D_z are displacements in the X, Y, and Z axes, respectively. This metric was chosen as it provides a simple yet informative measure of the amount of movement, which could be indicative of balance strategy or overall postural stability [27]. Greater total path lengths might indicate less efficient or more compensatory movements, suggesting poorer balance.

2.5.2. Jerk

Jerk, the rate of change of the acceleration, could indicate abrupt or uncontrolled movements, potentially signifying instability or difficulty in maintaining postural control. Jerk was calculated by differentiating pre-processed acceleration data as shown in Equation (4).

$$\begin{aligned} Jerk_x &= \frac{da_x}{dt} \\ Jerk_y &= \frac{da_y}{dt} \\ Jerk_z &= \frac{da_z}{dt} \end{aligned} \tag{4}$$

Higher jerk values may reflect less coordinated or controlled movements, which could increase the person's fall susceptibility [28].

2.5.3. Root Mean Square Accelerations and Angular Velocities

Apart from the linear accelerations that the IMUs provided, this study also evaluated the postural balance based on the angular velocities (ω), which refer to the rate of change of an object's rotational position with respect to time, measured around a specific axis. That is, ω quantifies how fast a sensor or a body part rotated and in which direction. For example, angular velocity along the X-axis represents side-to-side tilting, along the Y-axis represents forward and backward rotation, and along the Z-axis represents twisting of the trunk from the original standing posture.

Root Mean Square (RMS) values quantify the average magnitude of a fluctuating signal. From the collected and filtered signals of tri-axial linear accelerations and tri-axial angular velocities obtained from the IMUs, the RMS magnitudes of the acceleration and angular velocity were calculated as shown in Equations (5) and (6), respectively.

$$RMS_{Acceleration} = \sqrt{\text{Mean}((a_X)^2 + (a_Y)^2 + (a_Z)^2)} \tag{5}$$

$$RMS_{AngularVelocity} = \sqrt{\text{Mean}((\omega_X)^2 + (\omega_Y)^2 + (\omega_Z)^2)} \tag{6}$$

where a_X, a_Y, and a_Z are accelerations in the X, Y, and Z axes, respectively, and ω_X, ω_Y, and ω_Z are angular velocities in the X, Y, and Z axes, respectively. Higher RMS values provide insight into the overall intensity of movement and the amount of energy spent during a task.

2.5.4. Areas

To assess movement variability, we calculated three distinct area measures. These measures quantify the spatial dispersion of acceleration data.

Area under the acceleration magnitude curve, or area under the curve, was calculated using the trapezoidal method, as shown in Equation (7).

$$Area = \sum_{i=0}^{N-1} \frac{(a_i + a_{i+1})}{2} \times dt \tag{7}$$

where a_i and a_{i+1} are consecutive acceleration magnitudes, and dt is the time interval between samples. This measure quantifies the cumulative acceleration over time, providing

a temporal assessment of motion intensity. However, due to the discretization inherent in the trapezoidal method, this measure is more prone to errors than spatial metrics.

Ellipse area was calculated by fitting an ellipse to the acceleration data, using the standard deviations of the accelerations along the X and Y axes as the semi-axes to quantify the distribution of motion in the horizontal plane. The calculation of the ellipse area is shown in Equation (8).

$$Area_{ellipse} = \pi \times \sigma_X \times \sigma_Y \tag{8}$$

where σ_X and σ_Y represent the standard deviations of acceleration data on the X and Y axes, respectively. Mathematically, σ_X and σ_Y represent the spread of the data in each direction. These deviations correspond to the semi-major and semi-minor axes of the ellipse that best fits the data. This approach was expected to provide a robust indicator of data dispersion [29]. A larger ellipse area indicates greater dispersion of acceleration values, suggesting a wider range of motion or more complex movement patterns.

Bounding box area represents the minimal rectangular area that encloses all acceleration data points, calculated as shown in Equation (9).

$$Area_{box} = (max_X - min_X) \times (max_Y - min_Y) \tag{9}$$

where max_X, min_X, max_Y, and min_Y are the maximum and minimum acceleration values on the X and Y axes, respectively. Unlike the ellipse area, which provides a more precise representation of the distribution of acceleration data, the bounding box area has been known for its simplicity and computational efficiency, which is particularly suitable for real-time applications [30]. A larger bounding box area reflects a wider range of motion across a selected plane.

For example, Figure 2 presents the 2D projections of acceleration data in the XY plane during task execution. All in all, these area measures provide complementary perspectives on movement variability, capturing both the concentration of movement (ellipse area) and the overall range of motion across different planes (bounding box area and area under the curve).

It is worth noting that potential multicollinearity between these area measures was addressed during statistical analysis, and only one type of the three areas ended up being used in the prediction.

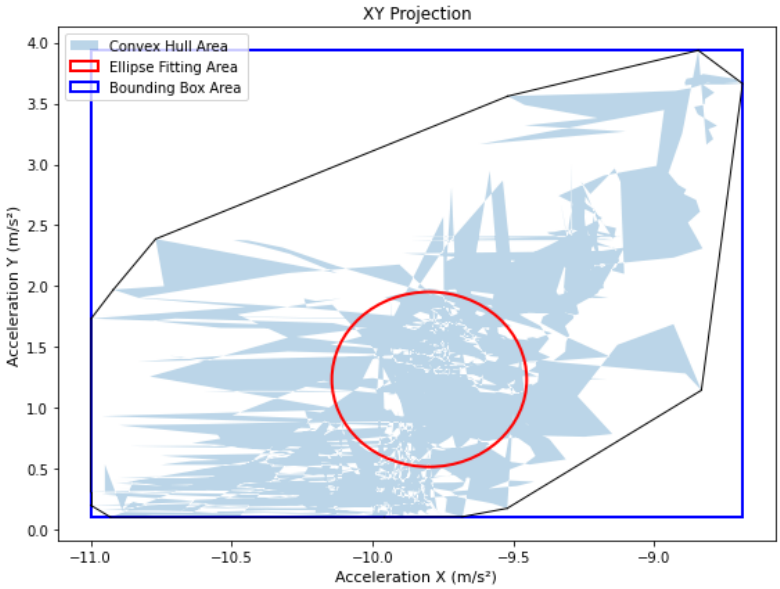

Figure 2. The 2D projection of accelerations in the horizontal (XY) plane; example for task 10. The black lines envelope the Convex Hall Area.

2.5.5. Volume

To capture the three-dimensional nature of movement, we introduced a novel volume metric that quantifies the space occupied by the acceleration data. This was calculated as the volume of the convex hull, which represents the smallest convex shape that encloses all acceleration data points [31], effectively capturing the boundaries of the movement space. The volume was calculated using Equation (10).

$$\text{Volume} = \frac{1}{3}\sum A_i \times h_i \tag{10}$$

where A_i is the area of the i-th face of the convex hull and h_i is its corresponding height. We utilized the *ConvexHull* class from the library *SciPy* in Python for efficient computation. This volume metric provides insights into movement complexity and adaptability, potentially reflecting a greater range of motion strategies used to maintain balance. A larger volume might indicate a more efficient postural control system, enabling exploration of a wider range of movements without losing balance. For instance, in post-stroke rehabilitation, an increase in trunk acceleration data volume over time could indicate improved postural control recovery [32]. This measure offers unique perspectives on balance assessment by capturing movement characteristics that may not be evident in traditional two-dimensional analyses.

Figure 3 shows a 3D visualization of the acceleration data points in all x, y, and z axes, the movement trajectory that was earlier computed through the application of Equation (2), and the calculated volume metric as described in Equation (10).

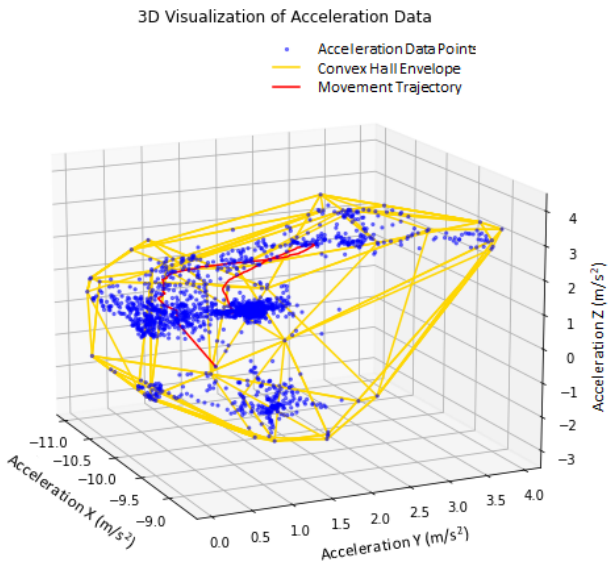

Figure 3. The 3D visualization of accelerations, movement trajectory, and convex hull volume; example for task 10.

2.6. Statistical Analysis

For the first objective to identify poor balance from the movement characteristics at the person's center of mass, we employed a logistic regression of the dichotomized BBS scores on the parameters derived from the lower back IMU data. The logistic regression model was formalized as shown in Equation (11).

$$logit(P) = \log\left(\frac{P}{1-P}\right) = \beta_0 + \beta_1 X_1 + \cdots + \beta_k X_k \tag{11}$$

where P is the probability of losing balance and $\beta_0, \beta_1, \ldots, \beta_k$ are coefficients of independent variables $X_0, X_1, \ldots, X_k$ representing movement characteristics derived from lower back IMU data. Each coefficient was evaluated at the significance level of 0.95.

To address multicollinearity and prevent overfitting, we examined the correlations among independent variables. The variables showing strong correlations with other variables were systematically eliminated from the logistic regression model, while we retained those strongly correlated with the binary outcome of poor balance.

For the second research objective to explore how sensor placement and task type affect the balance assessment, we analyzed data from different IMUs (head, torso, and lower back) separately as well as categorized the tasks as static or dynamic based on their nature. We then applied logistic regression to each combination of sensor and task type to identify predictive characteristics specific to each sensor location and task type.

3. Results

3.1. Descriptive Statistics and Correlation Analysis of IMU-Based Parameters

Table 2 presents descriptive statistics of movement characteristics extracted from IMU data collected from sensors on participants' lower back, torso, and head. The mean Z-acceleration for the head (-9.19 m/s², SD = 0.66) was close to the Earth's gravitational value (-9.81 m/s²), showing small vertical movement. In contrast, the standard deviation of Y-acceleration (2.53 m/s²) indicates greater variability in lateral head movements.

The acceleration area under the curve exhibited high variability, with significant standard deviations (e.g., 88,354,176.31 m/s for the lower back). These high values likely reflected the composite nature of this metric, integrating movement across all directions. The trapezoidal method used for calculation tends to produce larger values for repeated or oscillating movements. Standard deviations for bounding box and ellipse areas varied across body locations. These values indicated considerable variation in movement distribution across body regions.

Jerk values were small, indicating subtle rather than abrupt movement changes. The RMS angular velocity for the head showed a significant mean (25,390.09 rad/s) and high standard deviation (94,164.83 rad/s). This variability suggested considerable differences in movement strategies and postural stability among individuals.

The correlation matrix (Figure 4) further revealed significant relationships between these variables. The 2D-related characteristics (acceleration area under the curve, ellipse area, bounding box area) showed strong inter-correlations (coefficients 0.8–1.0). These associations indicated a close link between spatial dimensions and movement variability. Larger movement areas corresponded to greater variability across different surface measures, reflecting the sensitivity of area calculations to acceleration changes over time.

The RMS acceleration strongly correlated with the bounding box area (0.91), as greater acceleration variability led to wider dispersion of acceleration values in the XY plane. The total path length and the ellipse area had a strong correlation (0.83), which might have been due to the integration method used in the path calculation.

The volume metric correlates with both bounding box area (0.91) and ellipse area (0.83), suggesting that increased movement volume relates to larger movement areas in the horizontal plane and greater X–Y directional variability.

3.2. Identification of Poor Balance Indicators Derived from Data Measured at Lower Back

In the independent variable selection process for the logistic regression model, several IMU-derived characteristics were excluded to mitigate multicollinearity issues. The ellipse fitting area and bounding box area were omitted due to their high correlation ($r > 0.99$) with the area under the acceleration magnitude curve. RMS acceleration was eliminated due to its strong correlation ($r > 0.98$) with both area measures and mean acceleration X. Mean acceleration X was also excluded, owing to its high correlation with multiple variables. These exclusions aimed to reduce redundancy while retaining a diverse set of 1D, 2D, and 3D measures that capture distinct aspects of movement. As shown in Table 3, after adjusting for confounding factors (age, sex, weight, and height), key findings from the logistic regression include the following:

- The area under the acceleration magnitude curve was positively correlated with poor balance (coef = 0.78, $p = 0.002$), indicating that increased movement activity and more pronounced accelerations were associated with a higher risk of fall.
- RMS angular velocity showed a positive effect on poor balance (coef = 0.32, $p = 0.004$), suggesting that faster and more varied rotations may indicate balance instability.
- Total path length was negatively correlated with poor balance (coef = -1.82, $p = 0.0006$), implying that more extensive movement paths were associated with better stability.
- Movement volume was negatively correlated with poor balance (coef = -0.52, $p = 0.02$), suggesting that larger movement volumes indicate better balance control within our experimental context.

Table 2. Descriptive statistics (mean, standard deviation, minimum, Q1, Q3, and maximum) of the parameters from IMUs attached at the lower back, torso, and head.

Variable	Lower Back	Torso	Head
1D-based variables			
Mean acceleration X (m/s^2)			
Mean (SD)	1.94 (2.24)	1.98 (2.34)	0.53 (0.86)
[Q1, Q3]	[0.63, 3.38]	[0.85, 3.49]	[0.36, 0.93]
[Min, Max]	[−4.04, 7.12]	[−5.82, 5.64]	[−3.22, 3.21]
Mean acceleration Y (m/s^2)			
Mean (SD)	0.25 (1.20)	0.84 (0.46)	0.44 (2.54)
[Q1, Q3]	[−0.36, 1.03]	[0.61, 1.10]	[−1.23, 2.34]
[Min, Max]	[−3.30, 2.73]	[−1.83, 2.25]	[−5.55, 5.88]
Mean acceleration Z (m/s^2)			
Mean (SD)	−9.19 (0.66)	−9.14 (0.56)	−9.41 (0.61)
[Q1, Q3]	[−9.65, −8.99]	[−9.50, −8.91]	[−9.82, −9.25]
[Min, Max]	[−9.92, −6.68]	[−9.79, −6.04]	[−10.24, −7.14]
Jerk X (m/s^3)			
Mean (SD)	1.16×10^{-7} (6.55×10^{-7})	2.96×10^{-7} (7.66×10^{-7})	5.30×10^{-8} (2.06×10^{-7})
[Q1, Q3]	[-8.51×10^{-9}, 1.50×10^{-7}]	[1.75×10^{-8}, 3.81×10^{-7}]	[-4.29×10^{-9}, 1.12×10^{-7}]
[Min, Max]	[-2.42×10^{-6}, 5.70×10^{-6}]	[-3.14×10^{-6}, 2.80×10^{-6}]	[-5.20×10^{-7}, 8.87×10^{-7}]
Jerk Y (m/s^3)			
Mean (SD)	-2.23×10^{-8} (4.05×10^{-7})	-1.12×10^{-7} (4.43×10^{-7})	1.10×10^{-7} (5.32×10^{-7})
[Q1, Q3]	[-3.92×10^{-8}, 6.78×10^{-8}]	[-1.60×10^{-7}, 2.75×10^{-8}]	[-3.26×10^{-8}, 1.57×10^{-7}]
[Min, Max]	[-3.07×10^{-6}, 1.20×10^{-6}]	[-2.29×10^{-6}, 1.17×10^{-6}]	[-1.68×10^{-6}, 2.36×10^{-6}]
Jerk Z (m/s^3)			
Mean (SD)	-9.50×10^{-9} (2.15×10^{-7})	2.68×10^{-8} (2.42×10^{-7})	-3.60×10^{-8} (2.09×10^{-7})
[Q1, Q3]	[-9.55×10^{-9}, 1.12×10^{-8}]	[-2.98×10^{-8}, 8.56×10^{-9}]	[-3.88×10^{-8}, 8.19×10^{-9}]
[Min, Max]	[-1.11×10^{-6}, 8.63×10^{-7}]	[-8.88×10^{-7}, 1.23×10^{-6}]	[-1.10×10^{-6}, 1.04×10^{-6}]
2D-based variables			
Area under the curve (m/s)			
Mean (SD)	5.66×10^{7} (8.84×10^{7})	4.03×10^{7} (4.75×10^{7})	8.14×10^{7} (8.87×10^{7})
[Q1, Q3]	[1.08×10^{7}, 5.19×10^{7}]	[1.29×10^{7}, 4.84×10^{7}]	[1.83×10^{7}, 1.19×10^{8}]
[Min, Max]	[6.93×10^{5}, 5.55×10^{8}]	[2.29×10^{6}, 2.72×10^{8}]	[6.93×10^{5}, 4.87×10^{8}]
Ellipse fitting area (m^2/s^4)			
Mean (SD)	2.11 (3.09)	3.00 (5.98)	3.84 (4.97)
[Q1, Q3]	[0.093, 2.71]	[0.183, 2.88]	[0.750, 5.17]
[Min, Max]	[0.0031, 15.87]	[0.0117, 40.23]	[0.0491, 25.01]
Bounding box area (m^2/s^4)			
Mean (SD)	27.08 (40.54)	28.49 (29.46)	38.85 (36.69)
[Q1, Q3]	[2.67, 31.48]	[9.77, 36.59]	[11.05, 53.60]
[Min, Max]	[0.030, 311.65]	[0.448, 156.16]	[0.948, 182.40]
3D-based variables			
RMS acceleration (m/s^2)			
Mean (SD)	2.20 (1.60)	2.55 (2.44)	3.41 (2.19)
[Q1, Q3]	[0.92, 3.12]	[0.84, 3.65]	[1.79, 5.02]
[Min, Max]	[0.08, 7.67]	[0.14, 10.30]	[0.58, 9.91]
RMS angular velocity (rad/s)			
Mean (SD)	0.92 (0.33)	0.94 (0.35)	2.54×10^{4} (9.42×10^{4})
[Q1, Q3]	[0.77, 0.95]	[0.76, 1.01]	[0.87, 1.13]
[Min, Max]	[0.45, 3.29]	[0.60, 3.47]	[0.35, 4.16×10^{5}]
Total path length (m)			
Mean (SD)	1.19×10^{7} (3.37×10^{7})	7.47×10^{6} (1.88×10^{7})	1.18×10^{7} (2.58×10^{7})
[Q1, Q3]	[1.38×10^{4}, 4.59×10^{6}]	[1.36×10^{4}, 3.90×10^{6}]	[1.64×10^{4}, 8.04×10^{6}]
[Min, Max]	[93.69, 2.32×10^{8}]	[439.44, 1.03×10^{8}]	[161.80, 1.85×10^{8}]
Volume (m^3)			
Mean (SD)	72.67 (194.99)	38.86 (59.57)	70.92 (109.32)
[Q1, Q3]	[0.76, 58.90]	[3.41, 47.28]	[11.06, 69.49]
[Min, Max]	[0.0020, 1980.91]	[0.0660, 404.50]	[0.1431, 582.92]

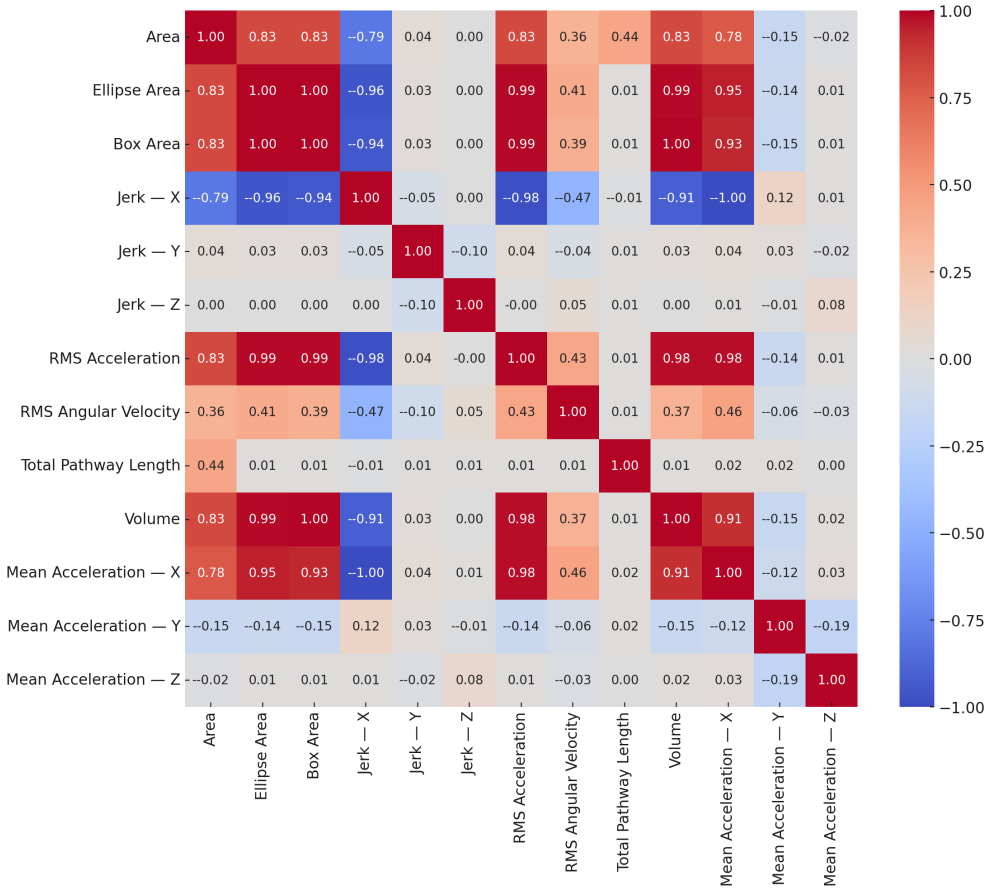

Figure 4. Correlation matrix of IMU-derived movement characteristics.

The final model included these variables along with jerk measures and selected mean accelerations, ensuring a comprehensive, yet non-redundant, representation of postural control characteristics. Finally, the model's AUC of 0.73 indicated an acceptable discriminative ability of this logistic regression model.

Table 3. Mean (SD) of the coefficients of the predictors of poor balance among various movement characteristics calculated from IMU data measured at the lower back.

Variable	Coefficient	Std. Error	*p*-Value
	Confounding Variables		
Age (years)	0.783	0.162	<0.0001
Sex (0 = female, 1 = male)	0.576	0.177	0.001
Weight (kg)	−0.542	0.197	0.006
Height (cm)	−0.038	0.196	0.84
	IMU-Derived Predictors		
Area under the curve (m/s)	0.780	0.254	0.002
Jerk X (m/s^3)	−0.250	0.146	0.08
Jerk Y (m/s^3)	0.054	0.139	0.69
Jerk Z (m/s^3)	−0.031	0.133	0.81
Mean acceleration Y (m/s^2)	0.145	0.141	0.31
Mean acceleration Z (m/s^2)	−0.110	0.123	0.38
RMS angular velocity (rad/s)	0.320	0.110	0.004
Total path length (m)	−1.820	0.528	0.0006
Volume (m^3)	−0.521	0.226	0.02

3.3. Influence of the Sensor Position on the Balance Predictors for Different Activity Types

The logistic regression models conducted separately for two activity types (static and dynamic) and different sensor placements revealed varying relationships between movement characteristics and balance. Table 4 summarizes predictors for each sensor location and task type combination. Our observations were as follows:

- For IMU attached to the head, vertical acceleration (Z-axis) was associated with better balance during static tasks but poorer balance during dynamic tasks, suggesting different control strategies for different task contexts. The overall results were different from when using the IMU at the lower back.
- For IMU attached at the torso, lateral acceleration (Y-axis) was negatively correlated with fall risk in dynamic tasks, while the movement volume and anterior–posterior jerk (X-axis) were positively correlated with fall risk.
- Larger movement volume from the IMU attached at the torso was associated with better balance in only dynamic tasks but not static ones. This was different from the results for the IMU at the lower back when pooling all tasks together.
- Total path length was an important predictive parameter when attaching the IMU to the torso, similarly to the lower back. However, the total path length could not help predict the risk of falls if the IMU was attached to the head.

These findings emphasize the importance of considering both sensor placement and task context when interpreting IMU data for balance assessment. These varying relationships between movement characteristics and balance across different body locations and task types suggest that a comprehensive balance assessment may incorporate multiple sensor locations, and that static and dynamic tasks should be analyzed separately.

Table 4. Confidence intervals of the balance predictors by sensor location and task type.

	Confidence Interval of the Coefficients		
Variable	Lower Back	Torso	Head
Static Tasks			
Area under the curve (m/s)	[−0.57, 0.07]	[−0.56, 0.10]	[−0.17, 0.31]
Jerk X (m/s^3)	[−0.21, 0.26]	[−0.37, 0.08]	[−0.17, 0.04]
Jerk Y (m/s^3)	[−0.13, 0.14]	[−0.43, 0.04]	[−0.12, 0.12]
Jerk Z (m/s^3)	[−0.18, 0.25]	[−0.15, 0.08]	[−0.11, 0.10]
Mean acceleration Y (m/s^2)	[−0.18, 0.05]	[−0.11, 0.15]	**[0.17, 0.51]**
Mean acceleration Z (m/s^2)	[−0.19, 0.05]	[−0.18, 0.08]	**[−0.30, −0.06]**
RMS angular velocity (rad/s)	[−0.13, 0.09]	[−0.22, 0.04]	[−0.16, 0.15]
Total pathway length (m)	**[0.001, 0.61]**	**[0.001, 0.65]**	[−0.19, 0.20]
Volume (m^3)	**[−0.24, −0.01]**	[−0.11, 0.12]	[−0.18, 0.13]
Dynamic Tasks			
Area (m/s)	[−0.28, 0.10]	[−0.17, 0.12]	[−0.22, 0.15]
Jerk X (m/s^3)	[−0.10, 0.11]	**[0.06, 0.33]**	[−0.19, 0.08]
Jerk Y (m/s^3)	[−0.13, 0.10]	[−0.12, 0.12]	[−0.06, 0.22]
Jerk Z (m/s^3)	[−0.12, 0.10]	[−0.16, 0.07]	[−0.03, 0.23]
Mean acceleration Y (m/s^2)	[−0.07, 0.14]	**[−0.23, −0.01]**	[−0.03, 0.31]
Mean acceleration Z (m/s^2)	[−0.09, 0.12]	[−0.15, 0.07]	**[0.06, 0.38]**
RMS angular velocity (rad/s)	[−0.13, 0.07]	[−0.16, 0.07]	[−0.04, 0.22]
Total pathway length (m)	[−0.09, 0.28]	[−0.08, 0.16]	[−0.08, 0.21]
Volume (m^3)	[−0.06, 0.15]	**[0.03, 0.28]**	[−0.10, 0.19]

4. Discussion

This section begins with providing the interpretation of our results, focusing on how various movement parameters influenced the fall risk. Then, we contextualize our findings with previous studies to present the validity and relevance of our study.

4.1. Factors Influencing Postural Balance

It is essential to account for individual factors that might have acted as confounders. These factors, including age, sex, weight, and height, could influence both the movement characteristics measured by the IMUs and the risk of falls. For instance, age was a significant predictor of fall risk (p-values < 0.0001), i.e., there was an increased risk of imbalance with advancing age. Similarly, sex and weight impacted postural stability (p-values = 0.001 and 0.006). By incorporating these confounding factors into our model, we were able to better isolate the specific effect of IMU-derived variables on fall risk as follows.

4.1.1. Area

The significant association between a larger area derived from the IMU at the lower back and an increased risk of poor balance could be explained by the dynamic nature of the 14 BBS tasks. These tasks demand constant postural adaptation and rapid reorganization of the motor responses. Similarly, Zhou et al. (2023) [33] found that balance control dysfunctions affected older adults' ability to maintain a safe gait. While their study specifically examined a gait, it highlighted the difficulties encountered during dynamic movements and the muscle tensions that disrupt stability. This aligns with the challenges observed in our study during dynamic BBS tasks, such as getting up from a chair, transferring between chairs, and bending to pick up an object.

4.1.2. RMS Angular Velocity

The RMS angular velocity, with its positive correlation (coef = 0.3182, p = 0.004), indicated that faster and more varied movements at the lower back are generally associated with an increased risk of poor balance. According to Donath et al. (2016) [34], older adults with high RMS angular velocities during balance tasks exhibited reduced postural stability. Although their study primarily focused on static balance tasks and used surface electromyography to measure muscle activity rather than kinematics directly, it reinforced the idea that high RMS angular velocity measures might be associated with deficiencies in the ability to maintain balance. Higher angular velocities may reflect excessive or poorly controlled postural adjustments, necessary to stabilize a less efficient neuromuscular system in older adults. Their findings and ours both suggested that RMS angular velocity could be a valuable metric for assessing balance control in the elderly. In practical terms, this could lead to the development of targeted interventions focusing on improving the control and smoothness of movements, particularly at the lower back, to enhance overall balance and reduce fall risk.

4.1.3. Total Path Length

Our analysis revealed an interesting association that a greater total path length at the lower back is linked to better stability, reflected by a perfect BBS score. That is, individuals with better balance were capable of exploring a larger movement space, as greater confidence in their postural abilities allowed them to move more freely without fear of losing balance. This observation aligns with Horak's [35] theories on the importance of confidence and motor competence for optimal performance on the BBS. A greater path length could indicate better flexibility, coordination, and motor planning, as well as efficient use of different movement strategies to maintain balance. According to Horak (2006) [35], confidence in one's postural abilities allows an individual to move with more assurance and explore a larger movement space without excessive apprehension.

The practical implication of this finding is significant as it suggests that balance training programs for the elderly should focus on not only stability but also movement confidence and range. This could involve exercises that encourage exploration of different movement patterns within a safe environment, potentially improving overall balance performance and reducing fall risk.

4.1.4. Volume

Based on our analysis, a larger movement volume measured at the lower back was correlated with better stability. This finding agreed with the previous observation on the total path length, i.e., that greater exploration of the movement space was associated with better balance. A larger volume could indicate a greater variability and a more diverse exploration of the movement in space during the BBS tasks. This ability of the participants to adapt their movements more flexibly and efficiently to the different task requirements was matched with a higher BBS score. Melecky et al. (2016) [36] supported this interpretation. They introduced the use of the convex hull volume, calculated directly from three-dimensional acceleration data, as a new method to quantify trunk postural stability; that is, they demonstrated the sensitivity of the volume metric to the participant's balance deficiency. Although their analysis focused on the movement of the trunk (equivalent to our torso measure), while our analysis used the lower back as the reference, both approaches shared the same fundamental principle of quantifying postural balance in the three-dimensional space explored through the convex hull volume of the acceleration data.

The volume metric provided a comprehensive measure in all three directions, offering insights into the overall mobility and adaptability of an individual's balance strategies. This finding on the volume metric has important implications for balance assessment in the elderly, similar to the total path length.

In conclusion, our findings suggest that while high-intensity, high-frequency movements often predict instability, the ability to control and modulate movement within a broader range is equally critical for balance. This comparative perspective broadens the potential applications of IMU-derived measures, emphasizing not only risk identification but also the development of intervention strategies that optimize balance through control-focused exercises.

4.2. Sensor Position and Balance in Relation to Activity Type

4.2.1. Lower Back

Our results during static tasks indicate that a larger movement volume was associated with better balance. This, once again, suggested that individuals with good balance explored a wider range of movement, effectively using the available space to find the optimal posture for stability. This corresponded to a previous study by Pourghayoomi et al. (2020) [37] using an indicator of postural stability based on the presence of the center of pressure in different rectangular functional areas to predict the intensity of fear of falling in patients with Parkinson's disease. This emphasized the importance of the volume metric in movement analysis for assessing postural stability.

In dynamic tasks, it is interesting to note that the measurement at the lower back did not reveal any statistically significant characteristics. This could indicate that while the sensor placement at the lower back as an approximate center of mass might play a crucial role in static balance, its contribution to assess dynamic balance was more subtle and probably integrated with the actions of other body segments, as suggested by Hansen et al. (2021) [38] on the reliability of IMU-derived balance parameters.

4.2.2. Torso

In our results during static tasks, a greater total path length measured at the torso suggested unsecured balance. This emphasized the fact that the trunk has a crucial role in maintaining vertical posture and stabilizing the center of mass. Likewise, Hosseinimehr et al. (2010) [39] demonstrated that the proprioception of trunk muscles, when disturbed by vibrations, affected dynamic postural control.

During dynamic tasks, trunk movements became more complex, and their influence on postural balance was more nuanced. The analysis revealed a complex interaction between trunk stability and mobility. Increased mean Y-acceleration was associated with better balance. This result may seem paradoxical, as another study by Ge et al. (2021) [40] showed that increased lower back acceleration was generally associated with poorer balance.

Notwithstanding, a previous study by Ringhof and Stein (2018) [41] on dynamic balance found that the balance skills depended on the tasks.

The interpretation when considering the IMU placed at the torso was different from when the IMU was placed at the lower back. This suggested that the two sensor positions were complementary. In addition, Doi et al. (2013) [42] demonstrated that the harmony of upper and lower trunk acceleration was a good predictor of falls in older adults, and that their measure of balance at the upper trunk, equivalent to the torso position in our study, could alone predict the incidence of falls well. Despite using different measures, their study is relevant to ours, as we also found that measures derived from torso IMUs were more discriminative than those from lower back IMUs.

4.2.3. Head

During static tasks, the head, essential for spatial perception and motor coordination, played a crucial role in maintaining balance. The higher mean acceleration on the medio-lateral axis (Y) indicated instability, often due to body oscillations or frequent postural adjustments. These results were confirmed by Noamani et al. (2023) [43] who found that measures such as RMS acceleration and frequency at the center of pressure particularly revealed balance impairment in older adults. On the contrary, increased acceleration on the vertical axis (Z) suggested better posture and more effective postural control. This result could be explained by the fact that higher vertical acceleration indicated a more stable postural alignment with the gravity.

In dynamic tasks, increased vertical acceleration (Z) was associated with reduced postural stability, suggesting a greater solicitation of the vestibular system and visual–motor reflexes. Extended head movements could provoke sensory conflicts, affecting sensory integration and motor coordination that are essential for stabilizing the body. Lacour et al. (2018) [44] found that patients with bilateral vestibular hypo-function rely more on extra-ocular signals from eye movements to stabilize their posture, especially in tasks requiring visual tracking.

All things considered, by providing a comparative assessment of these sensor locations, this study highlights the limitations of relying on a single IMU location to assess balance across varied activity types. This approach aligns with the need for task-specific balance metrics and demonstrates the value of integrating multiple sensor data points to create a comprehensive view of postural stability. Additionally, this study contributes to a more personalized approach to balance assessment, as different sensor placements may suit different individuals and balance challenges.

4.3. Practical Implications

The findings from our study can draw a complex picture of balance control in the elderly and the interplay between different aspects of motor function.

Firstly, our results pinpointed that postural balance is not simply about minimizing the movement, but rather the efficient and adaptive control of the movement. The findings regarding the area under the acceleration curve and the RMS angular velocity suggested that excessive or poorly controlled movements indicated balance issues. Meanwhile, the total path length and volume metrics showed that a larger range of controlled movement can be indicative of better balance. Thus, balance evaluation should incorporate measures that capture sufficiently diverse measures.

Secondly, the differences observed between static and dynamic tasks emphasized that balance control strategies are highly task-specific, which is aligned with the observations by Ringhof and Stein (2018) [41]. Therefore, comprehensive balance assessments should include a variety of tasks to capture the full spectrum of an individual's balance capabilities. Also, given the task-specific nature of balance control, interventions should be tailored to address individual deficits in specific types of tasks or movements.

Thirdly, as we found varying contributions of the IMUs placed at different body locations, it might be necessary to use several sensors together in balance assessment.

The measurement of each body part, i.e., lower back, torso, and head, could uniquely give insights about balance control, and their interactions could be important, as also mentioned by Doi et al. (2013) [42]. Using IMUs in multiple body locations, if possible, could be a promising approach for monitoring postural balance in daily life and for the early detection of balance issues for timely intervention.

Lastly, the positive associations between larger movement volumes, longer path lengths, and better balance scores supported Horak's [35] theories on the importance of confidence and motor competence in balance control. This suggests that balance interventions such as training should focus on not only stability but also encourage the exploration of movement to build confidence and competence.

4.4. Limitations and Considerations for Future Work

Despite the contributions of our study, several limitations should be acknowledged. Our sample size (N = 14) is relatively small, potentially limiting the generalizability of our findings. Gherbi and Thamsuwan (2024) [45] determined that at least 19 participants would be necessary to discriminate, with adequate statistical power, the participant's fall history using BBS scores. This suggested that our study may be underpowered, which could increase the risk of Type II errors and reduce the reliability of our results. Notwithstanding, our participant recruitment from the community with diversity in ethnicity, gender, age, and health background ensured this study's generalizability.

Moreover, IMUs could be subject to inherent measurement errors. These include drift, where small errors accumulate over time leading to gradually increasing inaccuracies, as well as noise, which can introduce random fluctuations in the data. To mitigate this, we only used the gyroscopes' data for one movement metric (the RMS angular velocity) and applied a low-pass filter to eliminate the noise in the acceleration data. Also, as such errors can affect the accuracy of long-term measurements [46], we chose a short-duration data collection where most tasks lasted for less than two minutes; thus, we expected these errors to be marginal.

Furthermore, our study focused on balance during specific BBS tasks, which may not fully capture all aspects of balance control in daily life. For example, task no. 12 (placing an alternate foot on a stool) was easier than actually climbing up or down the stairs. We did not account for factors such as environmental conditions (e.g., uneven surfaces, poor lighting), cognitive load (e.g., dual-task conditions), and fatigue, which can significantly influence balance performance [47]. For instance, cognitive load can divert attention from balance maintenance, while fatigue may impair muscle response times critical for maintaining stability.

Additionally, IMU data from the head and torso may be influenced by non-balance-related movements, requiring careful interpretation. These extraneous movements could potentially mask or mimic balance-related signals, complicating the analysis and potentially leading to misinterpretation of the data. Addressing these limitations in future research will be crucial for advancing the use of IMUs in balance assessments and fall prevention strategies for the elderly population.

Finally, the cross-sectional nature of our study limits our ability to assess changes in balance over time or the long-term predictive value of our IMU-derived metrics. A longitudinal study design would provide more robust evidence for the prognostic capabilities of these measures in fall risk assessment [48].

5. Conclusions

This study contributed to the assessment of postural balance through the use of IMUs. We developed a new movement volume metric, which was proven to be a sensitive indicator of balance. We also identified the lower back as a crucial measurement point for static balance assessment, with the movement volume and total path length serving as significant predictors of poor balance. Meanwhile, IMUs placed at the head and the torso

could provide complementary data, valuable for better understanding the balance under the dynamic activities.

Our research opens several avenues for future investigation. These include longitudinal studies to examine how IMU-derived balance measures change over time, the effect of balance training or other interventions on these measures, and the development of standardized protocols for IMU-based balance assessment. We envision the creation of user-friendly wearable devices, such as small unobtrusive sensors integrated into clothing, that could provide continuous balance monitoring and early warning systems for fall risk.

This research demonstrated the potential of IMUs to enhance continuous balance assessments in older adults, and ultimately the early identification of fall risks and personalized interventions. However, challenges may arise when auxiliary tasks are misaligned with the main task of balance assessment, potentially complicating data interpretation. To address this, future studies should consider designing protocols that isolate primary balance measurements or use task-specific filtering techniques to differentiate core balance data from auxiliary movements. Ensuring alignment between task demands and sensor placement could also help clarify the interpretation of IMU data in complex scenarios. Researchers and clinicians may build upon these findings and explore innovative applications of IMU technology in balance assessment and fall prevention to improve quality of life for the elderly population.

Author Contributions: Conceptualization, Y.N. and O.T.; methodology, Y.N. and O.T.; software, Y.N.; validation, Y.N. and O.T.; formal analysis, Y.N.; investigation, Y.N. and O.T.; resources, O.T.; data curation, Y.N. and O.T.; writing—original draft preparation, Y.N.; writing—review and editing, O.T.; visualization, Y.N.; supervision, O.T.; project administration, O.T.; funding acquisition, O.T. All authors have read and agreed to the published version of the manuscript.

Funding: This research was partially funded by the École de Technologie Supérieure, the new faculty start-up fund, and the Natural Sciences and Engineering Research Council of Canada, Discovery Grant Program (RGPIN-2022-0327).

Institutional Review Board Statement: This study was conducted in accordance with the Declaration of Helsinki, and approved by the Ethics Committee of École de Technologie Supérieure (Protocol No. H20221103 and date of approval 2 February 2023) for studies involving humans.

Informed Consent Statement: Informed consent was obtained from all subjects involved in the study.

Data Availability Statement: The data collected in this study were cleaned, organized, and made available in a public repository (https://github.com/ornwipa/imu-bbs, uploaded on 9 July 2024).

Acknowledgments: We extend our sincere gratitude to the individuals and organizations who made this research possible. Especially, the Notre-Dame-de-Grâce (NDG) Community Council provided crucial support in participant recruitment and community engagement. We are deeply grateful to all participants; their contributions were essential to this project's success. Special thanks go to Yasmine Gherbi for her dedication in recruiting participants and assisting with data collection, which was instrumental to the study's execution. We acknowledge the staff at the École de Technologie Supérieure, Department of Mechanical Engineering, for their facilities.

Conflicts of Interest: The authors declare no conflicts of interest. The funders had no role in the design of the study; in the collection, analyses, or interpretation of data; in the writing of the manuscript; or in the decision to publish the results.

References

1. Khalaf, M.A.K.; Değer, T.B. Evaluation of quality of life in the elderly who have fallen: Falling and quality of life in the elderly. *J. Surg. Med.* **2023**, *7*, 95–100. [CrossRef]
2. Parkkari, J.; Kannus, P.; Palvanen, M.; Natri, A.; Vainio, J.; Aho, H.; Vuori, I.; Järvinen, M. Majority of Hip Fractures Occur as a Result of a Fall and Impact on the Greater Trochanter of the Femur: A Prospective Controlled Hip Fracture Study with 206 Consecutive Patients. *Calcif. Tissue Int.* **1999**, *65*, 183–187. [CrossRef]
3. Smith, A.D.A.; Silva, A.O.; Rodrigues, R.A.P.; Moreira, M.A.S.P.; Nogueira, J.A.; Tura, L.F.R. Assessment of risk of falls in elderly living at home. *Rev. Lat.-Am. Enferm.* **2017**, *25*, e2754. [CrossRef]

4. Moreland, B.; Kakara, R.; Henry, A. Trends in Nonfatal Falls and Fall-Related Injuries Among Adults Aged ≥ 65 Years—United States, 2012–2018. *MMWR Morb. Mortal. Wkly. Rep.* **2020**, *69*, 875–881. [CrossRef] [PubMed]
5. Roe, B.; Howell, F.; Riniotis, K.; Beech, R.; Crome, P.; Ong, B.N. Older people and falls: Health status, quality of life, lifestyle, care networks, prevention and views on service use following a recent fall. *J. Clin. Nurs.* **2009**, *18*, 2261–2272. [CrossRef]
6. Harada, N.D.; Chiu, V.; Stewart, A.L. Mobility-related function in older adults: Assessment with a 6-minute walk test. *Arch. Phys. Med. Rehabil.* **1999**, *80*, 837–841. [CrossRef] [PubMed]
7. Hsu, Y.-C.; Zhao, Y.; Huang, K.-H.; Wu, Y.-T.; Cabrera, J.; Sun, T.-L.; Tsui, K.-L. A Novel Approach for Fall Risk Prediction Using the Inertial Sensor Data From the Timed-Up-and-Go Test in a Community Setting. *IEEE Sens. J.* **2020**, *20*, 9339–9350. [CrossRef]
8. Berg, K.O.; Wood-Dauphinee, S.; Williams, J.I.; Maki, B. Measuring balance in the elderly: Validation of an instrument. *Can. J. Public Health* **1991**, *83* (Suppl. S2), S7–S11.
9. Ness, B.M.; Taylor, A.L.; Haberl, M.D.; Reuteman, P.F.; Borgert, A.J. Clinical observation and analysis of movement quality during performance on the star excursion balance test. *Int. J. Sports Phys. Ther.* **2015**, *10*, 168.
10. August, G.J.; Gewirtz, A. Moving Toward a Precision-Based, Personalized Framework for Prevention Science: Introduction to the Special Issue. *Prev. Sci.* **2019**, *20*, 1–9. [CrossRef]
11. Karlsson, A.; Frykberg, G. Correlations between force plate measures for assessment of balance. *Clin. Biomech.* **2000**, *15*, 365–369. [CrossRef]
12. Ploof, G.; Alqahtani, B.; Alghamdi, F.; Flynn, G.; Yang, C.X. Center of Mass Estimation Using Motion Capture System. In Proceedings of the 2017 IEEE 15th Intl Conf on Dependable, Autonomic and Secure Computing, 15th Intl Conf on Pervasive Intelligence and Computing, 3rd Intl Conf on Big Data Intelligence and Computing and Cyber Science and Technology Congress(DASC/PiCom/DataCom/CyberSciTech), Orlando, FL, USA, 6–10 November 2017; pp. 287–292. [CrossRef]
13. De Groote, F. Validation of a smartphone embedded inertial measurement unit for measuring postural stability in older adults. *Gait Posture* **2020**, *82*, 146–152. [CrossRef] [PubMed]
14. Greene, B.R.; McGrath, D.; O'Neill, R.; O'Donovan, K.J.; Burns, A.; Caulfield, B. An adaptive gyroscope-based algorithm for temporal gait analysis. *Med. Biol. Eng. Comput.* **2010**, *48*, 1251–1260. [CrossRef] [PubMed]
15. Zougali, A.; Thamsuwan, O. Posture estimation in agriculture: Employing inertial measurement units and unscented Kalman filtering for trunk, shoulder, and elbow analysis. *IEEE Access* **2024**, *12*, 97332–97345. [CrossRef]
16. Nouredanesh, M.; Tung, J. Machine learning based detection of compensatory balance responses to lateral perturbation using wearable sensors. In Proceedings of the 2015 IEEE Biomedical Circuits and Systems Conference (BioCAS), Atlanta, GA, USA, 22–24 October 2015; pp. 1–4. [CrossRef]
17. Pickle, N.T.; Shearin, S.M.; Fey, N.P. A machine learning approach to targeted balance rehabilitation in people with Parkinson's disease using a sparse sensor set. In Proceedings of the 2018 40th Annual International Conference of the IEEE Engineering in Medicine and Biology Society (EMBC), Honolulu, HI, USA, 18–21 July 2018; pp. 1202–1205. [CrossRef]
18. Liuzzi, P.; Carpinella, I.; Anastasi, D.; Gervasoni, E.; Lencioni, T.; Bertoni, R.; Carrozza, M.C.; Cattaneo, D.; Ferrarin, M.; Mannini, A. Machine learning based estimation of dynamic balance and gait adaptability in persons with neurological diseases using inertial sensors. *Sci. Rep.* **2023**, *13*, 8640. [CrossRef]
19. da Silva, J.R.C. Machine Learning Applied to Fall Prediction and Detection Using Wearable Sensors. Ph.D. Dissertation, Faculdade de Engenharia da Universidade do Porto, Porto, Portugal, 2020.
20. Ghislieri, M.; Gastaldi, L.; Pastorelli, S.; Tadano, S.; Agostini, V. Wearable Inertial Sensors to Assess Standing Balance: A Systematic Review. *Sensors* **2019**, *19*, 4075. [CrossRef]
21. Pham, M.H.; Warmerdam, E.; Elshehabi, M.; Schlenstedt, C.; Bergeest, L.M.; Heller, M.; Haertner, L.; Ferreira, J.J.; Berg, D.; Schmidt, G.; et al. Validation of a Lower Back "Wearable"-Based Sit-to-Stand and Stand-to-Sit Algorithm for Patients with Parkinson's Disease and Older Adults in a Home-Like Environment. *Front. Neurol.* **2018**, *9*, 652. [CrossRef]
22. Shin, S.; Yoo, W. Inertial Measurement Unit-based Evaluation of Global and Regional Lumbar Spine and Pelvis Alignment in Standing Individuals with a Flat Lumbar Posture. *J. Manip. Physiol. Ther.* **2019**, *42*, 594–600. [CrossRef]
23. Scheltinga, B.L.; Usta, H.; Reenalda, J.; Buurke, J. Estimating Vertical Ground Reaction Force during Running with 3 IMUs. In Proceedings of the 8th World Congress on Electrical Engineering and Computer Systems and Science, Prague, Czech Republic, 28–30 July 2022. [CrossRef]
24. Janc, M.; Sliwinska-Kowalska, M.; Jozefowicz-Korczynska, M.; Marciniak, P.; Rosiak, O.; Kotas, R.; Szmytke, Z.; Grodecka, J.; Zamyslowska-Szmytke, E. A comparison of head movements tests in force plate and accelerometer based posturography in patients with balance problems due to vestibular dysfunction. *Sci. Rep.* **2021**, *11*, 19094. [CrossRef] [PubMed]
25. Deprá, P.P.; Amado, A.; van Emmerik, R.E.A. Postural Control Underlying Head Movements While Tracking Visual Targets. *Motor Control* **2019**, *23*, 365–383. [CrossRef]
26. Aich, S.; Chakraborty, S.; Sim, J.-S.; Jang, D.-J.; Kim, H.-C. The Design of an Automated System for the Analysis of the Activity and Emotional Patterns of Dogs with Wearable Sensors Using Machine Learning. *Appl. Sci.* **2019**, *9*, 4938. [CrossRef]
27. Strang, G. *Introduction to Linear Algebra*, 5th ed.; Wellesley-Cambridge Press: Wellesley, MA, USA, 2016.
28. Slaboda, J.C. Application of Jerk Analysis to a Repetitive Lifting Task in Patients with Chronic Lower Back Pain. Master's Thesis, University of Pittsburgh, Pittsburgh, PA, USA, 2004. Available online: http://d-scholarship.pitt.edu/id/eprint/7827 (accessed on 4 May 2023).

29. Wieczorek, B.; Kukla, M.; Warguła, Ł. Describing a Set of Points with Elliptical Areas: Mathematical Description and Verification on Operational Tests of Technical Devices. *Appl. Sci.* **2022**, *12*, 445. [CrossRef]
30. Stuckey, H.; Grijalva, N.; Carrillo, L.R.G.; Tang, W. A Single Camera Vision-Based Pose Tracking and Control System. In Proceedings of the 2023 IEEE 66th International Midwest Symposium on Circuits and Systems (MWSCAS), Tempe, AZ, USA, 6–9 August 2023; pp. 580–584.
31. De Berg, M.; Cheong, O.; Kreveld, M.V.; Overmars, M. *Computational Geometry: Algorithms and Applications*, 3rd ed.; Springer: Berlin/Heidelberg, Germany, 2008.
32. Barton, G.J.; Hawken, M.B.; Foster, R.J.; Holmes, G.; Butler, P.B. The effects of virtual reality game training on trunk to pelvis coupling in a child with cerebral palsy. *J. Neuroeng. Rehabil.* **2013**, *10*, 15. [CrossRef]
33. Zhou, J.; Liu, B.; Ye, H.; Duan, J.-P. A prospective cohort study on the association between new falls and balancing ability among older adults over 80 years who are independent. *Exp. Gerontol.* **2023**, *180*, 112259. [CrossRef]
34. Donath, L.; Kurz, E.; Roth, R.; Zahner, L.; Faude, O. Leg and trunk muscle coordination and postural sway during increasingly difficult standing balance tasks in young and older adults. *Maturitas* **2016**, *91*, 60–68. [CrossRef]
35. Horak, F.B. Postural orientation and equilibrium: What do we need to know about neural control of balance to prevent falls? *Age Ageing* **2006**, *35* (Suppl. S2), ii7–ii11. [CrossRef] [PubMed]
36. Melecky, R.; Socha, V.; Kutilek, P.; Hanakova, L.; Takac, P.; Schlenker, J.; Svoboda, Z. Quantification of Trunk Postural Stability Using Convex Polyhedron of the Time-Series Accelerometer Data. *J. Healthc. Eng.* **2016**, *2016*, 1621562. [CrossRef]
37. Pourghayoomi, E.; Behzadipour, S.; Ramezani, M.; Joghataei, M.T.; Shahidi, G.A. A new postural stability-indicator to predict the level of fear of falling in Parkinson's disease patients. *BioMed. Eng. OnLine* **2020**, *19*, 64. [CrossRef]
38. Hansen, C.; Beckbauer, M.; Romijnders, R.; Warmerdam, E.; Welzel, J.; Geritz, J.; Emmert, K.; Maetzler, W. Reliability of IMU-Derived Static Balance Parameters in Neurological Diseases. *Int. J. Environ. Res. Public Health* **2021**, *18*, 3644. [CrossRef]
39. Hosseinimehr, S.H.; Norasteh, A.A. The role of leg and trunk muscles proprioception on static and dynamic postural control. *Citius Altius Fortius* **2010**, *26*, 83.
40. Ge, L.; Wang, C.; Zhou, H.; Yu, Q.; Li, X. Effects of low back pain on balance performance in elderly people: A systematic review and meta-analysis. *Eur. Rev. Aging Phys. Act.* **2021**, *18*, 8. [CrossRef] [PubMed]
41. Ringhof, S.; Stein, T. Biomechanical assessment of dynamic balance: Specificity of different balance tests. *Hum. Mov. Sci.* **2018**, *58*, 140–147. [CrossRef] [PubMed]
42. Doi, T.; Hirata, S.; Ono, R.; Tsutsumimoto, K.; Misu, S.; Ando, H. The harmonic ratio of trunk acceleration predicts falling among older people: Results of a 1-year prospective study. *J. Neuroeng. Rehabil.* **2013**, *10*, 7. [CrossRef] [PubMed]
43. Noamani, A.; Riahi, N.; Vette, A.H.; Rouhani, H. Clinical Static Balance Assessment: A Narrative Review of Traditional and IMU-Based Posturography in Older Adults and Individuals with Incomplete Spinal Cord Injury. *Sensors* **2023**, *23*, 8881. [CrossRef] [PubMed]
44. Lacour, M.; Dosso, N.Y.; Heuschen, S.; Thiry, A.; Nechel, C.V.; Toupet, M. How Eye Movements Stabilize Posture in Patients With Bilateral Vestibular Hypofunction. *Front. Neurol.* **2018**, *9*, 744. [CrossRef] [PubMed]
45. Gherbi, Y.; Thamsuwan, O. Berg balance test for predicting a fall risk in older adults living at home: A preliminary study on the effect of pre-existing health conditions on postural balance. In Proceedings of the 22nd Triennial Congress Int. Ergonomics Association, Jeju, Republic of Korea, 25–29 August 2024.
46. Luinge, H.J.; Veltink, P.H. Measuring orientation of human body segments using miniature gyroscopes and accelerometers. *Med. Biol. Eng. Comput.* **2005**, *43*, 273–282. [CrossRef]
47. Zijlstra, A.; Mancini, M.; Chiari, L.; Zijlstra, W. Biofeedback for training balance and mobility tasks in older populations: A systematic review. *J. Neuroeng. Rehabil.* **2010**, *7*, 58. [CrossRef]
48. Lord, S.R.; Menz, H.B.; Tiedemann, A. A physiological profile approach to falls risk assessment and prevention. *Phys. Ther.* **2003**, *83*, 237–252. [CrossRef]